Journal of CO2 Utilization 66 (2022) 102289

Contents lists available at ScienceDirect

Journal of CO2 Utilization

journal homepage: www.elsevier.com/locate/jcou

Optimization of the integrated ORC and carbon capture units coupled to the refinery furnace with the RSM-BBD method

Reza Nazerifard [a], Mousa Mohammadpourfard [a,b,*], Saeed Zeinali Heris [a]

[a] Faculty of Chemical and Petroleum Engineering, University of Tabriz, Tabriz, Iran
[b] Department of Energy Systems Engineering, Izmir Institute of Technology, Izmir, Turkey

ARTICLE INFO

Keywords:
Refinery furnace
Organic Rankine cycle
CO_2 capture
Optimization
Response surface methodology
Economic

ABSTRACT

To recover waste heat and reduce the CO_2 emissions into the atmosphere, an integrated system of organic Rankine cycle and post-combustion carbon capture unit coupled with furnaces of a refinery located in Tabriz, East Azerbaijan, Iran has been presented. To assess the performances of the proposed system, thermodynamic and economic analyses are performed. The organic Rankine cycle was optimized by selecting the suitable working fluid with optimal operating conditions among the primary considered ones through multi-objective optimization. Then, the response surface methodology combined with the Box-Behnken design was employed to evaluate the effects of decision variables and their interaction on the CO_2 capture cost and attain the optimal conditions. The results indicate that the R-245fa is the best working fluids among the selected ones. According to the results, the flue gas inlet temperature into the absorber and lean loading are the terms of the model that have a significant impact on the output response. In the optimum setting of the decision variables, the CO_2 capture cost equals 81.60 $/t$_{CO2}$ and 81.90 $/t$_{CO2}$ for ORC+CC and DCC+CC processes, respectively. Furthermore, due to the absence of a turbine in the DCC+CC system, its equivalent work is 28 % higher than the ORC+CC system. Also, the amine regeneration energy is responsible for 91.47 % and 86.15 % of the variable operating cost of the optimal ORC+CC and optimal DCC+CC, respectively.

1. Introduction

The increase in energy consumption is one of the most significant challenges on the global scale, which is due to the growth in the worldwide population and the expansion of industrial activities. Globally, about 85 % of the produced energy comes from fossil fuels, which are declining [1]. In addition to concerns about the limitation on fossil fuel resources, emissions of greenhouse gases (GHG) which are mainly carbon dioxide (CO_2), methane (CH_4), nitrous oxide (N_2O), and water vapor (H_2O), is another challenge causing global warming, depletion of the ozone layer, acid rains, ice melting, rising sea levels, floods, climate changes, etc. Among these gases, CO_2 contributes to about 60 % of global warming and therefore needs special attention [2]. The average concentration of CO_2 in the atmosphere has risen about 50 m% from the beginning of the industrial revolution till now. That is why in recent decades, various meetings and conferences have been held to limit CO_2 emissions. Reports revealed that more than 60 % of global CO_2 emissions come from man-made sources, including power plants, refineries, petrochemicals, oil and gas processing, cement production, etc [3,4].

To reduce CO_2 emissions and its harmful and destructive effects, several methods have been proposed. Some of the most important of these methods are shown in Fig. 1. The first solution that can be considered is to improve the performance and efficiency of the processing units. One of the efficient methods in this field is waste heat recovery (WHR) of different industries. By converting these heat sources into electrical energy, the consumption of fossil fuels and carbon dioxide emissions can be significantly reduced. Studies show that the low-grade waste heat streams discharged into the atmosphere from the industries are more than half of the total heat produced and known as thermal pollution [5]. This waste heat is usually low in temperature, making it difficult to convert such heat into usable power through conventional methods. The main option for such a situation is the organic Rankine cycle (ORC) [6,7]. The operating principle of the ORC is similar to the Rankine cycle. The main difference is that it uses an organic working fluid with a higher molecular weight and lower boiling point and critical temperature than water [8]. Therefore, in the case of dealing with low-grade heat sources such as industrial waste streams, it provides better energy conversion. The most important advantage of the ORC is that it can be coupled with various systems such as geothermal, solar,

* Corresponding author at: Faculty of Chemical and Petroleum Engineering, University of Tabriz, Tabriz, Iran.
E-mail addresses: mohammadpour@tabrizu.ac.ir, mousamohammadpourfard@iyte.edu.tr (M. Mohammadpourfard).

https://doi.org/10.1016/j.jcou.2022.102289
Received 10 September 2022; Received in revised form 14 October 2022; Accepted 17 October 2022
Available online 24 October 2022

Nomenclature

ANOVA	Analysis of variance.
BBD	Box-Behnken design.
CC	Carbon capture.
CCUS	Carbon capture utilization and storage.
CRF	Capital recovery factor.
DCC	Direct contact cooling.
FOC	Fixed operating cost.
GHG	Greenhouse gas.
MEA	Monoethanolamine.
ORC	Organic Rankine cycle.
PCC	Post-combustion capture.
PEC	Purchase equipment cost.
RSM	Response surface methodology.
SHX	Series of heat exchangers.
TAC	Total annual cost.
TCI	Total capital investment.
TOC	Total operating cost.
VOC	Variable operating cost.
WHR	Waste heat recovery.

Nomenclature

A	Heat transfer area (m^2).
B	Bare module factor constants.
C	Cost ($).
CCC	CO_2 capture cost ($/tCO2).
CW	Cooling water.
F_{BM}	Bare module factor.
F_d	Design factor.
F_M	Material factor.
F_P	Pressure factor.
h	Mass enthalpy (kJ/kg).
hr	Annual operation hour.
HX	Heat exchanger.
i	Interest rate.
K	Cost constant.
a	Mass flow rate (kg/s).
n	plant lifetime (years).
P	Pressure (bar).
Q	Heat (kW).
T	Temperature (°C).
U	Overall heat transfer coefficient ($W/m^2.°C$).
W	Work (kW).
X	Capacity or size parameter.
x	Independent decision variable.
Y	Predicted response variable.

Greek letters

α	CO_2 loading.
ϵ	Error.
η	Efficiency.

Subscripts

annual	Annualized.
c	Compressor.
em	Emission.
en	Energy.
eq	Equivalent.
FG	Flue gas.
p	Pump.
pe	Petroleum.
RA	Rich amine.
reb	Reboiler.
ref	Reference.
regen	Regenerator.
st	Steam turbine.
sup	Degree of superheating.
t	Turbine.
th	Thermal.
wf	Working fluid.

biomass, and low-grade waste heat. This factor, along with other advantages such as high reliability and flexibility, simplicity of construction, and low operating and maintenance costs, has attracted lots of attention [9]. Behzadi et al. [10] analyzed the integrated waste-to-energy (WTE) power plant system of Tehran coupled with an ORC to recover the waste heat from the exhaust gas. With this new method, they could improve the net output power of the plant. Also, they reported that the energy and exergy efficiencies increased by 2.24 % and 1.87 %, respectively. A new system for exhaust flue gas waste heat recovery of the coal-fired boiler was designed by Jin et al. [11]. They used a high-temperature heat pump and organic Rankine cycle in their design and compared it with the conventional low-pressure economizer through thermodynamic and economic analysis. According to this investigation, this new design improves the deficiencies of the low-pressure economizers. Also, it can enhance the efficiency of waste heat utilization without reducing the recovery rate by producing approximately 410 kW additional power than a low-pressure economizer.

Fuel switching from fossil fuels to clean energy is another solution to help reduces the CO_2 emissions to the atmosphere. Renewable energy sources such as biomass, solar, wind, geothermal, and wave are examples of clean energy with a higher level of sustainability that do not emit CO_2. However, it should be noted that many renewable energy supplies are intermittent and have a small capacity compared to fossil fuel units, which results in a higher capital investment [12]. In addition, a lot of R&D work is needed to commercialize such technologies. Therefore, fossil fuels will remain the primary energy source for the short time.

Another option for limiting CO_2 emissions from fossil fuel combustion and mitigating its harmful impact on climate change is carbon capture utilization and storage (CCUS) technology. Since reducing the dependency on fossil fuels for industrial large-scale seems unlikely in the near future, therefore CCUS technologies are the only practical way to limit CO_2 emissions. According to Fig. 1, the main categories of carbon capture processes are post-combustion capture (PCC), pre-combustion capture, and oxy-fuel combustion capture. In the pre-combustion method, CO_2 is captured prior to the combustion of the fuel. For this, the fuel is converted into the mixture of H_2 and CO_2 by the gasification process, and then CO_2 is removed from this gas mixture, and H_2 combusted as a fuel in the presence of the air. In oxy-fuel combustion, the fuel is combusted with oxygen instead of air. As a result, the flue gas has a high concentration of CO_2 due to a lack of nitrogen. This method requires lots of energy to extract oxygen. Contrary to pre-combustion, in post-combustion capture, CO_2 is separated from the flue gas stream after the combustion [13]. Among these three main categories for carbon capture, PCC is the most widely used process for many reasons, which the most significant one is the capability to integrate this system into existing plants as a retrofit unit without any fundamental changes in the main process [14,15]. Several technologies, including physical and chemical absorption, adsorption, cryogenic, biological, and membrane processes are available for PCC. Due to the low concentration of CO_2 and high flue gas volume, only chemical absorption by amine-based solvent can be commercially implemented on an industrial large-scale for CO_2

separation [16,17]. A 30 wt% (5 kmol/m^3) monoethanolamine (MEA) is the benchmark amine solvent for PCC. However, this process consumes high amounts of thermal energy for solvent regeneration, which increases the operating cost of the process. In addition, MEA began to degrade at temperatures above 120 °C, which reduces its absorption capacity [18–20]. To improve the amine-based chemical absorption process to reduce its operating cost and implement it on the industrial scale to mitigate the CO_2 emissions into the environment, three approaches have been proposed [20–22]. The first approach is the development of new solvents or blends. Nwaoha et al. [23] techno-economically analyzed CO_2 capture from the flue gas of a cement plant using an AMP-PZ-MEA blend solution and compared it with the single MEA. The simulation results show that the regeneration energy for the MEA is higher than the blend. Also, the capture cost of the AMP-PZ-MEA blend is 17% lower than MEA. In another study, 30–50 wt % aqueous blends of AMP-PZ solvents was considered for carbon capture from the flue gas stream of a coal-fired power plant [24]. The results of this study revealed that with a blend of (18 wt% AMP+17.5 wt% PZ), the required energy for regeneration could be reached to 3.7 GJ/t_{CO2}. Zhang et al. [25] investigated different amine molar ratios of MEA-MDEA-PZ blends as a solvent for carbon capture. They concluded that these blends reduce energy consumption by 15.22–49.92 % compared to MEA. The second approach is the modification of the process to a new configuration. Examples of process modifications is absorber intercooling (AI), lean vapor compression (LVC), stripper overhead compression (SOC), stripper split feed (SSF), cold solvent split (CSS), and rich vapor recompression (RVR). To reduce the MEA regeneration energy, Jung et al. [26] suggest alternative configurations by combining RVR and CSS. They concluded that their new combining configuration could reduce the reboiler heat requirement from 3.44 GJ/t_{CO2} to 2.75 GJ/t_{CO2}. Zhao et al. [27] analyzed the performance of PCC for a 650 MW power plant using MDEA-PZ as a solvent according to absorber intercooling, simple and advanced rich-split, and stripper interheating. They found that these configurations are efficient and improve the process efficiency. Also, the reboiler heat duty can reduce by 27.7 % with a developed configuration at optimum operating conditions. The third approach for chemical absorption-based PCC is optimizing the operating condition, since the performance of the chemical processes, especially the carbon capture unit, depends strongly on the operating conditions. A parametric sensitivity of CO_2 capture from a coal-fired power plant is investigated by Nwaoha et al. [28] by considering five independent variables that has a significant impact on different dependent variables. They observed that the reboiler temperature and lean amine flow rate have the highest effect on the amine regeneration energy. They also concluded that the amine regeneration energy contributed 82.5 % of the variable operating expenditure. The influence of various operating conditions like lean solvent loading, lean solvent temperature, absorption percentage, solvent concentration, and reboiler pressure on the performance of PCC from fossil fuel-fired power plant has been studied by Abu-Zahra et al. [29]. The results of their investigation show that the CO_2 lean loading has a major effect on the energy consumption of the capture system. They also suggest a 23 % reduction in reboiler thermal energy by using a 40 wt% MEA.

From the literature review in the previous paragraphs, it can be concluded that most of the researcher has focused only on one of the methods for CO_2 emissions reduction. However, it seems more studies and investigations are needed in this field. So, the novel contribution of this work is to improve the available studies by integrating the first and the third approaches to reducing carbon emissions, which can produce electrical power besides CO_2 emissions reduction. Therefore, this study was performed to analyze the performance of coupling the ORC and MEA-based CO_2 capture with refinery furnaces flue gas with a low

Fig. 1. methods of reducing CO_2 emissions.

concentration of CO_2. Moreover, since the optimal operating conditions can reduce energy consumption and carbon capture cost, using the multi-objective optimization and RSM-BBD method, the proposed system is optimized to obtain optimal operating conditions. Section 2 presents a detailed description of the proposed system and its subsystems. Section 3 describes the mathematical relations for thermodynamic and economic analysis of the system, as well as adopted assumptions. Also, the optimization method, including decision variables and objective functions, is presented in this section. In Section 4, the obtained results from the simulation and optimization are discussed. Finally, the conclusions of the study are given in Section 5.

2. System description

An overview of the proposed integrated system is shown in Fig. 2. As can be seen, this system consists of a refinery furnace, an organic Rankine cycle, and an amine process for carbon capture. The flue gas of the refinery furnaces has a high temperature and this heat source can be used to generate electricity. By doing this, the consumption of fossil fuels and CO2 emissions can be reduced. Also, the temperature of the flue gas decreases to become suitable for the carbon capture process. After this step, the flue gas enters the absorber of the capture unit, where 90 % of CO2 is chemically absorbed by 30 wt% MEA. The detailed description of each subsystem is explained below. For the design and simulation of the proposed system, Aspen HYSYS v10 is used with two fluid packages. A rate-based "Acid Gas - Chemical Solvents" fluid package is used for simulation of the carbon capture unit, while "Peng-Robinson" is adapted for the rest of the units, including furnace, ORC, and compression units. Then, Design Expert v13 is adapted to optimize the proposed system based on RSM-BBD.

2.1. Furnace

In industrial processes, especially in refineries, endothermic reactions occur at high temperatures. The heat required to carry out these reactions is provided by the direct combustion of fossil fuels in furnaces. In this study, the waste heat of flue gas is extracted as the heat source for power generation by ORC and then, its CO_2 is captured by an amine unit. To accurately design of the proposed system, the actual industrial values of a refinery located in Tabriz, East Azerbaijan, Iran, will be used as a case study. Table 1 shows the composition of the fuel gas used for combustion in the furnace. For simulation of the furnace in Aspen HYSYS, the Gibbs reactor module based on the minimization of the Gibbs free energy concept, was used. The outlet of this reactor corresponds with the exhaust flue gas from the stack of the furnace, which is used as a heat source in the organic Rankine cycle and then in the carbon capture unit.

Table 1
Molar composition of the refinery fuel gas used for combustion in the furnace.

Composition	Molar fraction
CH_4	0.798
C_2H_6	0.058
C_3H_8	0.015
i-C_4H_{10}	0.009
n-C_4H_{10}	0.010
i-C_5H_{12}	0.005
n-C_5H_{12}	0.003
H_2	0.071
N_2	0.027
CO_2	0.004

2.2. Organic rankine cycle

As stated before, flue gases from furnaces have high temperatures and contain a large amount of heat energy. Therefore, to use this energy, an organic Rankine cycle can be employed. The ORC system consists of six basic components, including a series of heat exchangers (SHX) (preheater, evaporator, and superheater), a turbine, a generator linked to the turbine, a condenser, a vessel, and a pump. The subcooled working fluid is pumped to the tube sides of the SHX from the vessel and heated by the flue gas and vaporizes into the superheat. Then, this superheat working fluid with a pressure of 30 bar, enters the turbine, where it expands and its enthalpy and pressure decrease. The turbine is linked to a generator where the electric power is produced. Afterward, the low-pressure working fluid flows into the condenser and condenses to the initial state by cooling water.

In addition to suitable operating conditions, the working fluid also has a remarkable influence on the thermal performance of ORC systems, and selecting of this working fluid is one of the most critical considerations in the design step [30]. The selected working fluid also affects investment and operating cost, and the right choice can help both maximizing efficiency and minimizing costs. Therefore, it is crucial to choose suitable organic fluid according to the heat source conditions. A variety of organic fluids such as Hydrocarbons (HC), Hydrofluorocarbons (HFC), Hydrochlorofluorocarbons (HCFC),

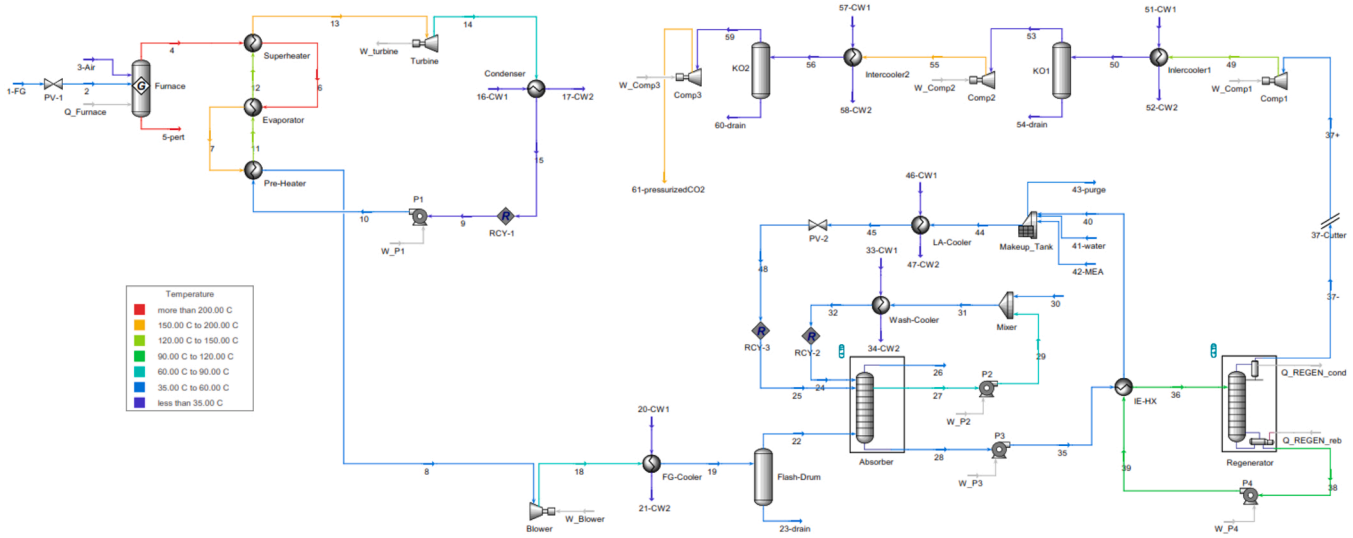

Fig. 2. process configuration of the integrated system in Aspen HYSYS.

Hydrofluoroolefin (HFO), Alcohols, Amines, etc. can be used as working fluid in the ORC systems [31]. Since there are many candidates for working fluid, it is necessary to make a primary selection according to the following principles to reduce the workload:

- The working fluid should have a slight environmental impact which can be described by the Ozone Depletion Potential (ODP), the Global Warming Potential (GWP), and the Atmospheric Lifetime (ALT) indices;
- Proper thermal and chemical stability during the cycle to avoid decomposition, which increases the fouling resistance on heat exchanger surfaces and changes in fluid thermodynamic properties;
- Good safety characteristics in the system include non-flammable, non-corrosive, non-toxic, non-corrosive;
- Low cost and easy availability.

Another vital aspect to consider is the thermodynamic behavior of the working fluid, which depends on the slope of the saturation vapor curve in a T-s diagram and can be divided into three categories as dry fluids with a positive slope ($dT/ds > 0$), wet fluids with a negative slope ($dT/ds < 0$) and isentropic fluids with a nearly vertical curve ($dT/ds \rightarrow \infty$). Because of the liquid droplet impingement, wet fluids can cause damage to the turbine blades once they expand through the turbine, while dry and isentropic fluids are in superheated areas even after passing through the turbine and therefore, this problem does not arise.

According to these principles, four primary working fluid candidates were selected to choose the optimal one for power generation from waste heat of refinery furnaces flue gases. Table 2 shows the properties of these working fluids.

2.3. Carbon capture

In this study, the amine process is designed to capture 90 % of the CO_2 in the flue gas of a refinery furnace with a purity of > 98 wt%. According to Fig. 2, the outlet flue gas from the pre-heater of the ORC enters a gas blower to overcome the pressure drop in the further unit. Typically, the absorber tower operates at 40–50 °C, and therefore, a cooling of the flue gas is needed, which is mainly done by direct contact cooling (DCC). But in this study, most of the thermal energy of the flue gas is extracted through the ORC and only a tiny percentage remains. Therefore, the flue gas is cooled with cooling water in one heat exchanger (FG-cooler) to adjust its inlet temperature to the amine unit. The flue gas is then fed into the absorber column from the bottom, while the lean 30 wt% MEA enters from the top. Inside the packed bed absorber column, the solvent moves downward and counter-currently interacts with upward flowing flue gas. This contact between the flue gas and the solvent causes a series of chemical reactions as follows [32]:

$$2H_2O \leftrightarrow H_3O^+ + OH^- \quad (1)$$

$$CO_2 + OH^- \rightarrow HCO_3^- \quad (2)$$

$$H_2O + HCO_3^- \leftrightarrow H_3O^+ + CO_3^{2-} \quad (3)$$

$$HCO_3^- \rightarrow CO_2 + OH^- \quad (4)$$

$$MEA + H_2O + CO_2 \rightarrow MEACOO^- + H_3O^+ \quad (5)$$

$$MEACOO^- + H_3O^+ \rightarrow MEA + H_2O + CO_2 \quad (6)$$

$$MEAH^+ + H_2O \leftrightarrow MEA + H_3O^+ \quad (7)$$

According these reactions, CO_2 is absorbed into the aqueous MEA solvent to form a rich solvent. To reduce the solvent losses and recover the solvent from the treated flue gas, a washing section is considered at the top of the absorber column above the lean aqueous solvent feed location. In this section, the treated flue gas contacts the wash water, which captures most of the MEA from the gas phase. The water is drawn from the liquid collector located on the top of the absorber packing section and after mixing with the deionized water and cooling to 40 °C, is recycled to the top of the washing section. After passing from the washing section, the treated gas is vented to the atmosphere from the top of the column.

The bottom stream of the absorber, which is rich solvent, is pumped by the rich pump to the lean/rich heat exchanger in which it is heated by the hot regenerated lean solvent from the bottom of the regeneration column and then fed into the stripper (regenerator) column. Inside this column, CO_2 is stripped from the solvent through stripping steam, which is generated at the bottom of the column. Using low-pressure steam (LPS), the heat is supplied to the reboiler, where partial evaporation of the lean solvent generates the required stripping steam. The overhead product of the column, i.e., CO_2 and water vapor, enters a condenser where its water vapor is condensed at 35 °C and fed back to the column, while CO_2 is compressed through a multi-stage compression unit with intercooling up to the desired pressure. From the bottom of the stripper column, the hot lean solvent is pumped backed to the absorber column by the lean pump. But first, it gets cool in the lean/rich heat exchanger, and after mixing with water and amine make-up streams, is further cooled down in a trim cooler and then enters the top of the absorption section of the absorber column.

3. System modeling and analysis

As aforementioned in the previous section, the industrial values of a refinery located in Tabriz, East Azerbaijan, Iran, are used in this study. The main goal of the present work is to optimize the process of waste heat recovery from the flue gas and reduction of CO_2 emissions by achieving 90 % of CO_2 capture with a purity of > 98 wt%. Therefore, this plant is capable of capturing > 150,000 t_{CO2}/year. The pre-described integrated refinery furnaces with ORC system and post-combustion carbon capture unit are developed using Aspen HYSYS v10 and the thermophysical properties of the streams were calculated by using two different fluid packages. “Acid Gas - Chemical Solvents” fluid package with rate-based calculation is used for simulation of carbon capture unit. In contrast “Peng-Robinson” fluid package is used to calculate the thermodynamic properties of the furnace, ORC, and carbon compression. In the simulation, the absorber and regenerator columns were configured to have 22 stages, in which stages 1 and 2 from the top are considered as washing section and stages 3–22 as absorbing/stripping sections. The stage packing height for both columns was set at 0.5 m, which leads to the overall packing height becoming 1 m for the washing section and 10 m for the absorbing/stripping sections. A 3 kPa pressure drop was considered for the absorber, while for the regenerator, this value equals 5 kPa. In both columns, flooding was set as 80 %

Table 2
Properties of primarily selected working fluids for ORC.

Working fluid	Chemical formula	ODP	GWP	ALT	T_c (°C)	P_c (bar)	Fluid type	Price ($/kg)
R-1234ze	$C_3H_2F_4$	0	6	–	109.4	36.62	dry	26.0
R-236ea	$C_3H_2F_6O$	0	710	–	139.2	34.12	dry	19.6
R-245fa	$C_3H_3F_5$	0	950	7.2	154.1	36.40	dry	12.4
R-600a	C_4H_{10}	0	20	0.019	134.7	36.40	dry	4.68

as this condition, in conjunction with the amine flow rate, determines the required diameter of the columns. Also, for both absorber and regenerator, including column internals and washing sections, structured packing Sulzer Mellapak 250Y is used. Furthermore, the modified HYSIM inside-out solving algorithm with an adaptive damping factor and error tolerance of 10^{-6} was selected in the solver for both columns. The details of the "Acid Gas - Chemical Solvents" fluid package can be found in [16,21,33]. The following assumptions are adopted in the simulation step of the system:

- The system operates under steady-state conditions.
- The pressure losses throughout the pipelines are ignored and a 5 % pressure drop is applied to the heat exchangers (both tube and shell sides).
- The outlet working fluid from the condenser of the ORC is subcooled liquid with temperature and subcooling degrees of 35 °C and 5 °C, respectively.
- Cooling water is used as cooling media with a temperature of 25 °C and pressure of 3.5 bar. The outlet temperature of the cooling water is 35 °C.
- The flue gas leaves the ORC with a temperature of 55 °C to prevent condensation.
- Constant adiabatic efficiency of 85% is considered for all rotating equipment.
- All components of the system are thermally insulated. Therefore, the heat losses from the pipelines and equipment are assumed to be zero.
- Ambient conditions are 25 °C and 1 atm.

In this section, mathematical relations to assess the performance of the proposed system were developed.

3.1. Thermodynamic analysis

The energy performance of this integrated system can be evaluated based on the first law of thermodynamics, which is specified by energy efficiency. The energy or first law efficiency of the organic Rankine cycle can be defined as follow:

$$\eta_{en,ORC} = \frac{W_{net,ORC}}{Q_{SHX}} = \frac{W_{t,ORC} - W_{p,ORC}}{Q_{SHX}} \tag{8}$$

In addition to the ORC, it is necessary to evaluate the energy performance of the overall proposed system, which includes the thermal energy used in the reboiler of the capture unit as well as the electrical power of the rotating equipment. Since these types of energy are not the same, there is a need to combine them into one total equivalent work. Eq. (9) shows the four main contributors to the total equivalent work [34]:

$$W_{eq} = W_{th} + W_c + W_p - W_{t,ORC} \tag{9}$$

where W_{eq} is the total equivalent work, W_{th} is the solvent regeneration heat work, W_c is the sum of electrical energy used to run the compressors and blower, W_p is the sum of consumed electrical energy by pumps, and $W_{t,ORC}$ is the electrical energy produced in the ORC. The solvent regeneration heat work indicates how much electrical power can be produced by a steam turbine with the same amount of steam consumed in the reboiler. According to Eq. (10), this parameter can be calculated using the Carnot efficiency method:

$$W_{th} = Q_{reb}\left(1 - \frac{T_C}{T_H}\right)\eta_{st} \tag{10}$$

Where Q_{reb} is the reboiler heat duty, T_C is the steam condensation temperature in the steam turbine of the refinery utility unit that provides the electrical energy of the refinery, T_H corresponds to the reboiler steam temperature and η_{st} is the steam turbine efficiency.

3.2. Economic analysis

To successfully design a new system, it is necessary to estimate the required investment and prices of the final products. Therefore, in addition to evaluating the thermodynamic performance of the proposed system, economic analysis should also be conducted. To assess the economic performance of the system, the total capital investment (TCI) and total operating cost (TOC) should be calculated. After estimation of TCI and TOC, evaluation of the economic feasibility of the proposed system can be done by using various indices.

3.2.1. Total capital investment

The total capital investment is based on the purchase equipment cost (PEC) estimation as well as the initial ORC working fluid and amine solution. There are several methods to estimate the PEC. The most accurate way is to obtain it from the vendor. The following reliable way is to use data from previously purchased equipment with the same type, material and capacity. Another way is to use cost correlations and graphs that are available to kinds types of equipment in the literature. Here, the third method is used to estimate the PEC, which is a common approach in the literature and can be calculated according to the following general correlation [35]:

$$\log C_{PEC} = K_1 + K_2 \log(X) + K_3[\log(X)]^2 \tag{11}$$

Where C is the cost, X is the capacity or size parameter of the equipment (area (m^2) for heat exchangers, power (kW) for pump, turbine, generator, compressor and driver, volume (m^3) for vessel). The cost of the generator's gearbox is estimated as 40 % of the generator cost [36]. After calculating the purchased cost of equipments, the bare module cost can be evaluated based on pressure and material correction:

$$C_{BM} = C_{PEC}F_{BM} \tag{12}$$

$$F_{BM} = B_1 + B_2F_MF_P \tag{13}$$

$$\log F_P = C_1 + C_2 \log(P) + C_3[\log(P)]^2 \tag{14}$$

where F_{BM} is the bare module factor, B_1 and B_2 are bare module factor constants, F_M is the material factor, F_P is the pressure factor and P is the pressure in barg. The values of constants for various equipment are given in Table 3. Furthermore, to consider the inflation effect on equipment costs, the CEPCI (Chemical Engineering Plant Cost Index) was adopted. The purchase cost of each equipment in the year 2020 can be estimated by:

$$C_{BM,2020} = C_{BM,ref} \times \frac{CEPCI_{2020}}{CEPCI_{ref}} \tag{15}$$

where $CEPCI_{2020}$ is 596.2 and $CEPCI_{ref}$ is 394.3 for 2001.

According to Eq. (11), the PEC of the heat exchangers is based on the heat transfer area. In this study, the logarithmic mean temperature difference (LMTD) method is used to determine the areas of heat exchangers:

$$A = \frac{Q}{U\Delta T_{LMTD}} \tag{16}$$

where Q is the exchanger duty and U is the overall heat transfer coefficient. The values of Q and ΔT_{LMTD} are extracted directly from the Aspen HYSYS simulation, while the values of U for each heat exchanger are estimated from [37]. It should be noted that in the case of the regenerator reboiler, the cost was multiplied by a design factor (F_d) of 1.35 [23]. Also, in evaluating the volume of the absorber and regenerator, it was assumed that the packing in the column is 70% of the total column height [38].

Besides estimating the PEC, it is necessary to estimate the price of ORC working fluid as well as the initial amine solution. The required working fluid to fill the piping conveying the working fluid and the equipments of the ORC, is considered to be 1.5 times the volume of the

Table 3
Values of constants for general correlation of PEC [35].

Equipment	K_1	K_2	K_3	C_1	C_2	C_3	B_1	B_2	F_M	F_{BM}
Pre-Heater	4.3247	-0.303	0.1634	0.03881	-0.1127	0.08183	1.63	1.66	2.72	–
Evaporaor	4.3247	-0.303	0.1634	0.03881	-0.1127	0.08183	1.63	1.66	2.72	–
Superheater	4.3247	-0.303	0.1634	0.03881	-0.1127	0.08183	1.63	1.66	2.72	–
Condenser	4.3247	-0.3030	0.1634	–	–	–	1.63	1.66	1.37	–
FG-Cooler	4.3247	-0.3030	0.1634	–	–	–	1.63	1.66	2.72	–
Wash-Cooler	4.3247	-0.3030	0.1634	–	–	–	1.63	1.66	1.37	–
IE-HX	4.3247	-0.3030	0.1634	–	–	–	1.63	1.66	2.72	–
LA-Cooler	4.3247	-0.3030	0.1634	–	–	–	1.63	1.66	2.72	–
Regen-Condenser	4.3247	-0.3030	0.1634	–	–	–	1.63	1.66	2.72	–
Regen-Reboiler	4.3247	-0.3030	0.1634	–	–	–	1.63	1.66	2.72	–
Intercooler1	4.3247	-0.3030	0.1634	0.03881	-0.1127	0.08183	1.63	1.66	2.72	–
Intercooler2	4.3247	-0.3030	0.1634	0.03881	-0.1127	0.08183	1.63	1.66	2.72	–
P1	3.3892	0.0536	0.1538	-0.3935	0.3957	-0.00226	1.89	1.35	1.51	–
P2	3.3892	0.0536	0.1538	–	–	–	1.89	1.35	1.51	–
P3	3.3892	0.0536	0.1538	–	–	–	1.89	1.35	2.27	–
P4	3.3892	0.0536	0.1538	–	–	–	1.89	1.35	2.27	–
Turbine	2.7051	1.4398	-0.1776	–	–	–	–	–	–	3.5
Generator	4.1055	0.0570	0.0797	–	–	–	–	–	–	1.5
Comp1	2.2897	1.3604	-0.1027	–	–	–	–	–	–	7.0
Comp1 Driver	2.9508	1.0688	-0.1315	–	–	–	–	–	–	1.5
Comp2	2.2897	1.3604	-0.1027	–	–	–	–	–	–	7.0
Comp2 Driver	2.9508	1.0688	-0.1315	–	–	–	–	–	–	1.5
Comp3	2.2897	1.3604	-0.1027	–	–	–	–	–	–	7.0
Comp3 Driver	2.9508	1.0688	-0.1315	–	–	–	–	–	–	1.5
ORC Vessel	3.5565	0.3776	0.0905	–	–	–	1.49	1.52	1	–
Flash Drum	3.4974	0.4485	0.1074	–	–	–	2.25	1.82	3.1	–
Absorber	3.4974	0.4485	0.1074	–	–	–	2.25	1.82	3.1	–
Regenerator	3.4974	0.4485	0.1074	–	–	–	2.25	1.82	3.1	–
Regen-Reflux drum	3.5565	0.3776	0.0905	–	–	–	1.49	1.52	3.1	–
KO1	3.4974	0.4485	0.1074	–	–	–	2.25	1.82	3.1	–
KO2	3.4974	0.4485	0.1074	–	–	–	2.25	1.82	3.1	–

ORC vessel [39]. The price of ORC working fluids is given in Table 2, while for estimating the required cost to purchase the 30 wt% MEA solution, the method presented in the [23] is used.

3.2.2. Total operating cost

The total operating cost (TOC) consists of the fixed operating cost (FOC) and the variable operating cost (VOC). The fixed operating cost includes the costs of maintenance, labor, local taxes and insurance, administration, laboratory, supervision, etc. For ORC, it was assumed as 1.65 % of TCI [40], while for the capture and compression units, it was considered as 3 % of the TCI [19]. The variable operating cost is the annual sum of utility and make-up stream costs. The total electricity consumption is equal to the sum of the electricity consumed by compressors, pumps and blower minus the electricity produced in the ORC. Table 4 shows the unit costs used for the evaluation of the VOC.

3.2.3. Economic indices

Once these costs is obtained, the total capital investment (TCI) and total operating cost (TOC) can be calculated according to the following relation:

$$TCI = \sum C_{BM,i} + C_{fluid} \tag{17}$$

$$TOC = FOC + VOC \tag{18}$$

The total annual cost (TAC) is the bases for economic analysis and can be calculated by:

$$TAC = TCI_{annual} + TOC \tag{19}$$

where TCI_{annual} is the annualized total capital investment which can be determined by multiplying the TCI and capital recovery factor (CRF):

$$TCI_{annual} = TCI \times CRF \tag{20}$$

$$CRF = \frac{i(1+i)^n}{(1+i)^n - 1} \tag{21}$$

where n is plant lifetime (30 years) and i is the interest rate (10 %).

One of the most important indices in the analysis of the PCC unit is the CO_2 capture cost (CCC), and with this index, the data obtained from different works can be compared with each other. This index can be expressed as the total annual cost divided by the total mass of captured CO_2:

$$CCC = \frac{TAC}{Mass\ \ of\ \ captured\ \ CO_2} \tag{22}$$

Table 4
unit costs of process utilities and make-up streams [41].

Working fluid	Price (unit)
MEA	2200 ($/ton)
DM water	1.130 ($/ton)
Cooling water	0.013 ($/ton)
electricity	13.28 ($/GJ)
Steam	16.80 ($/GJ)

3.3. Optimization

Production of the desired product with minimum energy consumption and cost has always been considered by the chemical industries. Therefore, properly setting of process parameters and operating conditions is necessary to achieve this goal. There is usually more than one factor affecting the energy consumption and cost of the process. Accordingly, to accurately examine the proposed system of coupling ORC and MEA-based carbon capture to refinery furnaces, it is necessary to optimize the operating conditions. So, the operating conditions of both ORC and carbon capture units should be optimized.

Optimization of the ORC has two steps. In the first step, according to the energy efficiency, the working fluid is selected and then, in the second step, the operating condition is optimized by the multi-objective optimization method. Here, the energy efficiency and total annualized

cost of the ORC are considered as thermodynamic and economic objective functions that changes according to the degree of superheating (T_{sup}):

$$Maximize: \quad F_1(x) = \eta_{en,ORC} \tag{23}$$

$$Minimize: \quad F_2(x) = TAC_{ORC} \tag{24}$$

to solve this multi-objective problem, the linear weighted evaluation function method is adopted as follows for thermo-economic optimization of the ORC:

$$F(x) = \alpha F_1(x) + \beta F_2(x) \tag{25}$$

where α and β are weight coefficients of the objective function and can be evaluated by:

$$\alpha = \frac{\left(F_2^1 - F_2^2\right)}{\left(F_1^2 - F_1^1\right) + \left(F_2^1 - F_2^2\right)} \tag{26}$$

$$\beta = 1 - \alpha \tag{27}$$

the values of F_1^1, F_1^2, F_2^1 and F_2^2 are described in [42].

After the ORC system has been optimized by selecting the appropriate working fluid and degree of superheating, it is time to optimize the entire system of coupling ORC and MEA-based carbon capture, for which CO_2 capture cost has been selected as the objective function. Here, the optimization methodology adapted is response surface methodology (RSM). RSM, based on the design of experiments (DoE), is a set of mathematical and statistical techniques that are useful for modeling and analyzing problems in which the response is affected by several variables and it can optimize this response. This method reduces the number of trials and is able to estimate the effects of each variable as well as their interaction on the response variable. The generalized quadratic polynomial model describes the behavior of the response variable in the RSM can be shown as:

$$Y = \beta_0 + \sum_{i=1}^{k} \beta_i x_i + \sum_{i=1}^{k-1} \sum_{j=1+1}^{k} \beta_{ij} x_i x_j + \sum_{i=i}^{k} \beta_{ii} x_i^2 + \in \tag{28}$$

here, Y is the predicted response variable, β_0, β_i, β_{ij} and β_{ii} are the coefficients for intercept, linear, quadratic, and interactive terms, respectively, x_i and x_j are the independent variables, k is the number of variables, and ϵ is the error term.

To develop this regression equation between selected decision and output response variables, the analysis of variance (ANOVA) by Design expert v13 is used. In the present study, a three-level four-factor Box-Behnken design (BBD) which consists of 29 runs was employed. The considered decision variables are: lean amine loading (α_{lean}), flue gas inlet temperature into the absorber (T_{FG}), rich amine inlet temperature into the regenerator (T_{RA}) and regenerator reboiler pressure (P_{regen}). Table 5 summarizes the considered decision variables (factors) with their levels. The response variable is the CO_2 capture cost.

3.4. Validation

As stated earlier in the previous sections, the proposed system of this study consists of refinery furnaces, an organic Rankine cycle, and a post-combustion carbon capture unit. So, all of them need to be validated for further studies. To validate the furnace simulation, the values obtained from the simulation are compared with actual industrial values. The results of Table 6 show that the Gibbs reactor can accurately predict the conditions of the furnace. As a result, the composition and condition of stack flue gas can be used for power generation and capture unit with confidence. Also, to validate the developed model for ORC simulation, the literature data were used and the comparisons of the reference data [43] with the simulation results are presented in Table 6. It is observed that there is a good agreement with a minor deviation between these data. Therefore, the developed model for ORC is reliable. In the case of the carbon capture unit, the results from the simulation are compared to the pilot plant data [44]. Fig. 3 shows the comparison between pilot plant data with simulation results for absorber and regenerator temperature and CO_2 mass fraction in liquid phase profiles. It is evident that the presented model satisfactorily predicts the performance with a minor deviation.

Table 5
Decision variables with their levels.

Symbol	Decision variable	Level 1 (−1)	Level 2 (0)	Level 3 (+1)
A	α_{lean} (mol_{CO2}/mol_{amine})	0.16	0.185	0.21
B	T_{FG} (°C)	40	47.5	55
C	T_{RA} (°C)	102	104.5	107
D	P_{regen} (bar)	1.62	1.72	1.82

4. Results and discussion

In this section, the results of coupling the organic Rankine cycle and MEA-based carbon capture with the refinery furnaces are discussed.

4.1. ORC working fluid and condition selection

The performance results of the ORC as a function of the degree of superheating in the outlet stream of SHX are shown in Fig. 4. The energy efficiency of the ORC can be obtained from Eq. (8). Since the conditions of the flue gas at the inlet and outlet of the SHX are constant, the value of the denominator of the efficiency relation is unchanged. So, $\eta_{en,ORC}$ will change with the variation of the numerator, i.e., $W_{net,ORC}$. As a result, the variation trend of efficiency for each working fluids is similar to that of the net power output of the same working fluid. The $W_{net,ORC}$ is the difference between turbine power production and pump power consumption. These power production and consumption are proportional to the cycle mass flow rate and the enthalpy differences of turbine and pump inlet and outlet streams:

$$W_{net,ORC} = W_t - W_p = \dot{m}_{wf}\left(h_{13} - h_{14}\right) - \dot{m}_{wf}\left(h_{10} - h_9\right) \tag{29}$$

According to this figure, increasing the degree of superheating causes to increase in enthalpy differences and a decrease in the mass flow rate of the working fluid. At a low degree of superheating, enthalpy difference is a dominant factor in energy efficiency, while at a high degree of superheating, the mass flow rate of the working fluid is prominent. Consequently, the energy efficiency curve has a maximum value.

In addition to the energy efficiency, Fig. 4 also shows the total annualized cost of each working fluid. According to Eq. (19), TAC consists of the annualized total capital investment and the total operating cost. Increasing the degree of superheating causes to an increase in the SHX and turbine cost, which are the main contributor to the capital investment of the ORC. Contrary, the mass flow rate of the cooling water decreases by increasing the degree of superheating. The overall tradeoff

Table 6
comparison of the industrial/reference data with simulation results.

Parameter	Industrial or Ref.[43]	This study	Error%
Furnace validation			
Flue gas temperature (°C)	269.2	270	0.2972
N_2 molar fraction	0.733	0.7313	0.2319
O_2 molar fraction	0.042	0.041	2.3810
CO_2 molar fraction	0.077	0.0787	2.2078
H_2O molar fraction	0.148	0.149	0.6757
ORC validation			
Mass flow rate (kg/s)	1.06	1.033	2.5472
Net power (kW)	49.04	49.73	1.4070
Thermal efficiency (%)	19.46	19.74	1.4388
Condenser duty (kW)	202	199.55	1.2129

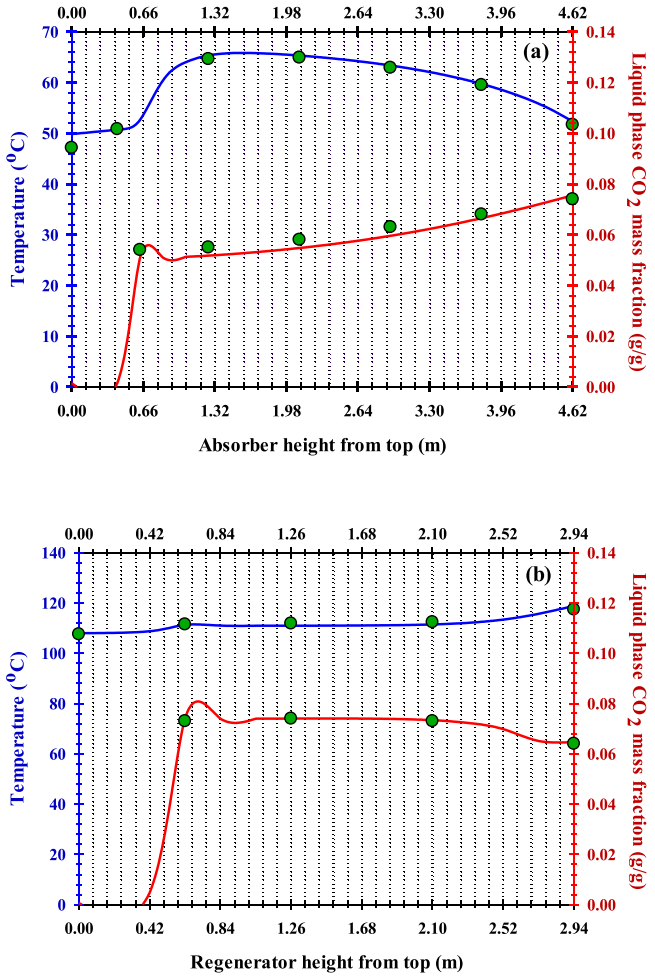

Fig. 3. simulation results of carbon capture unit from Aspen HYSYS versus pilot data: (a) absorber, and (b) regenerator.

between these two conflicting factors emerged as a minimum point in the TAC diagram.

After performing thermodynamic and economic analyses, it is necessary to select the most suitable working fluid and its operating condition. For this purpose, the results obtained from Fig. 4 are used. From this figure, it is evident that the energy efficiency of the R-245fa is higher than the others. Therefore, this working fluid is selected to perform further operating condition optimization using Eq. (25). The result of the multi-objective optimization for the ORC is presented in Fig. 5. This figure shows the relation of $F(x)$ versus T_{sup}. It can be observed that $F(x)$ increases and then decreases with an increasing the degree of superheating, revealing the existence of an optimal value for T_{sup}, which is equal to 15.8 °C. At this point, the energy efficiency and TAC of the ORC are equal to 13.44 % and 784,444.7 $/year, respectively. So, in this way, the optimal working fluid and degree of superheating are selected for the ORC to couple with the carbon capture unit. At this optimal state, the operating conditions of the main streams of the ORC are listed in Table 7.

4.2. ANOVA results

As aforementioned in the previous section, the RSM-BBD method is used to study the effect of different variables on CO_2 capture cost and optimization of the whole process. The designed runs (29 runs) using the BBD method and the obtained responses are shown in Table 8. Also, the ANOVA in Design Expert v13 is used to check the adequacy of the regression model terms and estimate the coefficients of the response

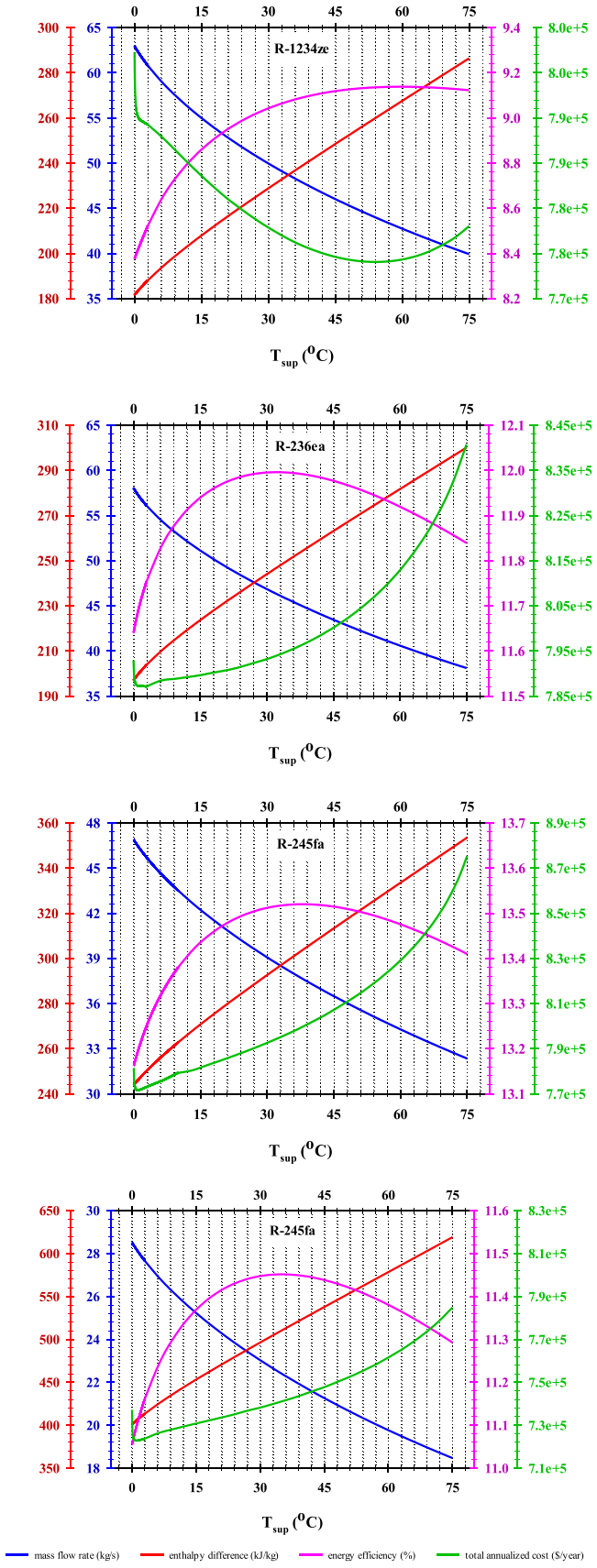

Fig. 4. performance results of the ORC as a function of T_{sup} for various working fluids.

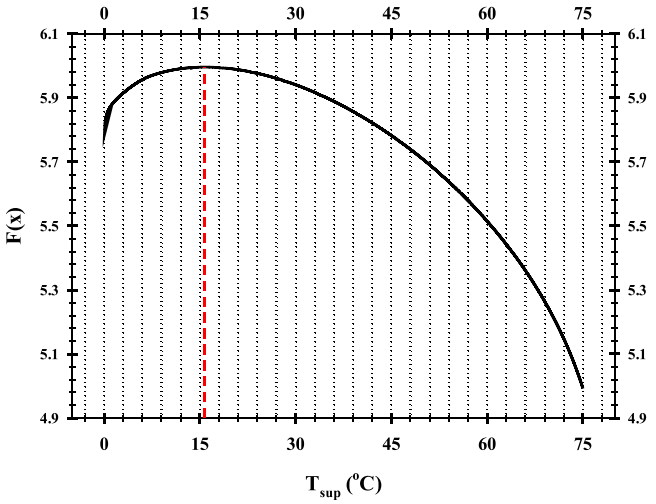

Fig. 5. results of multi-objective optimization of the ORC.

Table 7
main streams conditions of the ORC.

	Stream No.	m (t/h)	T (°C)	P (bar)
Inlet flue gas to the ORC	4	169.07	270	1
Outlet flue gas from the ORC	8	169.07	55	0.95
Pump inlet	9	151.34	35	2.49
Pump outlet	10	151.34	36.49	31.58
Turbine inlet	13	151.34	159	30
Turbine outlet	14	151.34	86.34	2.62

variable. The ANOVA results are summarized in Table 9.

In the ANOVA table, the significances of the terms are statistically determined by the p-values and F-values. Generally, if the p-values are less than 0.001 (p-value<0.001), then the model terms are highly significant. The p-values less than 0.05 indicate that the model terms are significant, while p-values greater than 0.1 means the insignificancy of the model terms. Also, the higher F-value, the greater the significance of the effect of the terms. Therefore, the higher F-value and lower p-value, the more importance of the corresponding coefficient. From Table 9, the model F-value of 125.27 and p-value< 0.0001 implies that the model is significant with a very low probability of error. Furthermore, in this case, A, B, C, D, AC, AD, CD, A^2, and B^2 are significant model terms. The most significant term of the model is the flue gas inlet temperature into the absorber (T_{FG}), with the highest F-value. The goodness of fit of the quadratic polynomial model was determined by R^2 values. A higher

Table 9
results of ANOVA for CO_2 capture cost.

Source	Sum of squares	df	Mean square	F-value	p-value
Model	160.68	14	11.48	125.27	< 0.0001
A	25.45	1	25.45	277.80	< 0.0001
B	88.23	1	88.23	962.97	< 0.0001
C	3.46	1	3.46	37.77	< 0.0001
D	8.07	1	8.07	88.09	< 0.0001
AB	0.125	1	0.125	1.36	0.2624
AC	0.7258	1	0.7258	7.92	0.0138
AD	4.24	1	4.24	46.25	< 0.0001
BC	0.1876	1	0.1876	2.05	0.1744
BD	0.0013	1	0.0013	0.0137	0.9083
CD	0.6866	1	0.6866	7.49	0.0160
A^2	25.11	1	25.11	274.04	< 0.0001
B^2	7.66	1	7.66	83.59	< 0.0001
C^2	0.209	1	0.209	2.28	0.1532
D^2	0.349	1	0.349	3.81	0.0713
Residual	1.28	14	0.0916		
Lack of fit	1.28	10	0.1283		
Pure error	0	4	0		
Cor total	161.97	28			
Standard deviation = 0.3027			R^2 = 0.9921		
Mean = 85.12			Adjusted R^2 = 0.9842		
Coefficient of variation = 0.3556			Predicted R^2 = 0.9544		
			Adeq Precision = 44.0712		

Table 8
corresponding designed runs and response values.

Std.	Run	α_{lean}	T_{FG}	T_{RA}	P_{regen}	CO_2 capture cost ($/$t_{CO2}$)		Error%
						HYSYS	RSM	
7	1	0.185	47.5	102	1.82	84.4572	84.2256	0.2743
16	2	0.185	55	107	1.72	86.6838	86.9074	0.2580
25	3	0.185	47.5	104.5	1.72	83.6814	83.6829	0.0018
4	4	0.21	55	104.5	1.72	88.0208	87.8158	0.2330
20	5	0.21	47.5	107	1.72	83.5486	83.4105	0.1653
2	6	0.21	40	104.5	1.72	82.5384	82.7454	0.2508
9	7	0.16	47.5	104.5	1.62	89.5333	89.1881	0.3855
1	8	0.16	40	104.5	1.72	85.3090	85.3047	0.0050
23	9	0.185	40	104.5	1.82	81.6995	81.4872	0.2598
6	10	0.185	47.5	107	1.62	84.7695	84.7918	0.0263
21	11	0.185	40	104.5	1.62	82.8695	83.0919	0.2685
3	12	0.16	55	104.5	1.72	91.4984	91.0821	0.4550
8	13	0.185	47.5	107	1.82	82.5342	82.3230	0.2560
17	14	0.16	47.5	102	1.72	87.1462	87.3973	0.2881
28	15	0.185	47.5	104.5	1.72	83.6814	83.6829	0.0018
11	16	0.16	47.5	104.5	1.82	85.1660	85.4893	0.3796
5	17	0.185	47.5	102	1.62	85.0353	85.0372	0.0022
29	18	0.185	47.5	104.5	1.72	83.6814	83.6829	0.0018
22	19	0.185	55	104.5	1.62	88.2260	88.5513	0.3687
27	20	0.185	47.5	104.5	1.72	83.6814	83.6829	0.0018
24	21	0.185	55	104.5	1.82	86.9851	86.8756	0.1259
18	22	0.21	47.5	102	1.72	85.4241	85.3364	0.1027
13	23	0.185	40	102	1.72	82.6756	82.5575	0.1428
26	24	0.185	47.5	104.5	1.72	83.6814	83.6829	0.0018
19	25	0.16	47.5	107	1.72	86.9746	87.1752	0.2307
10	26	0.21	47.5	104.5	1.62	84.4345	84.2167	0.2579
15	27	0.185	40	107	1.72	82.0046	81.9167	0.1073
14	28	0.185	55	102	1.72	88.2210	88.4145	0.2194
12	29	0.21	47.5	104.5	1.82	84.1845	84.6351	0.5353

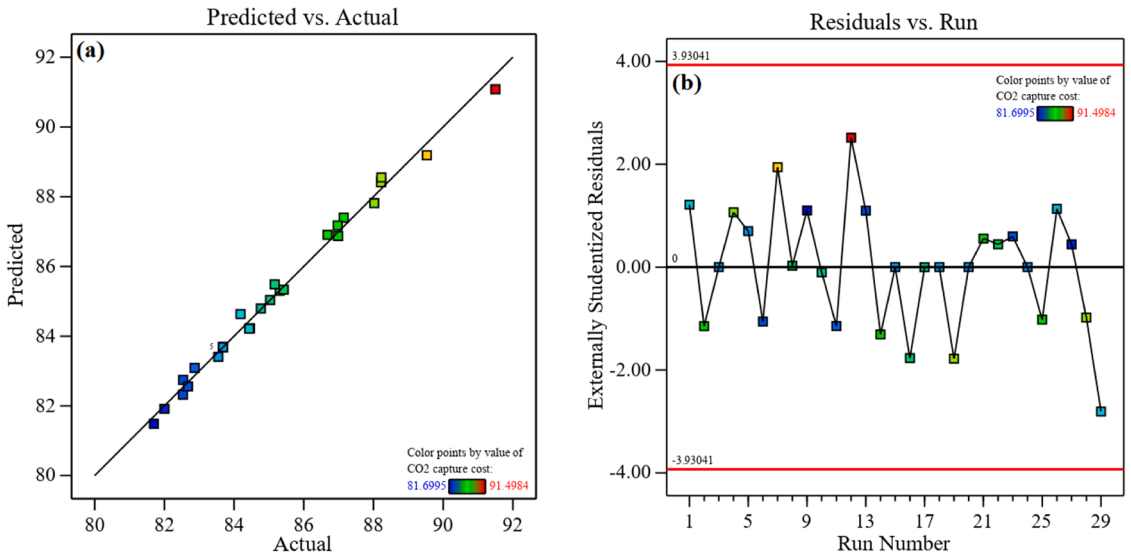

Fig. 6. – the RSM-BBD plots for (a) predicted values of CCC vs. actual Aspen HYSYS values and (b) externally studentized residuals vs. run number.

value of R^2 represents that the fitted model can predict the response variable with high accuracy. In this model, the R^2 value of 0.9921 indicates a good fit of data obtained from the Aspen HYSYS. Also, there is no problem with either the data or the model, as the difference between adjusted R^2 and predicted R^2 is less than 0.2. Additionally, the Adeq. Precision of 44.0712 (greater than 4) demonstrates that the RSM model has a solid signal to be used for optimization.

From these discussions, it can be concluded that the predicted model of CO_2 capture cost by RSM has adequate precision and can be used for further investigation. Based on regression results, the obtained quadratic polynomial function for the CO_2 capture cost is described as follows:

$$\begin{aligned} CCC = {} & 281.24597 - 1174.13375\alpha_{lean} - 0.051551T_{FG} - 1.55733T_{RA} + 10.13486P_{regen} \\ & -0.942706\alpha_{lean}T_{FG} - 6.81569\alpha_{lean}T_{RA} + 411.72422\alpha_{lean}P_{regen} - 0.011550T_{FG}T_{RA} \\ & -0.023658T_{FG}P_{regen} - 1.65722T_{RA}P_{regen} + 3147.92025\alpha_{lean}^2 + 0.019318T_{FG}^2 \\ & +0.028720T_{RA}^2 + 23.19720P_{regen}^2 \end{aligned} \quad (30)$$

Fig. 6(a) shows the plot of predicted versus actual values for CO_2 capture cost. It is clear that the real and predicted values for output response are close to each other, as shown in Table 8. The plot of the residuals versus the run order is depicted in Fig. 6(b). According to this figure, data related to run #29 differs more from its predicted values than others. However, there is no cause of problem due to it being within the red control lines.

4.3. Effects of operating conditions

Fig. 7 shows the perturbation plot of all the decision variables. This diagram, in which the response is plotted by changing only one decision variable over its range while holding all the other variables constant, helps to compare the effects of all the variables at a specified point. In a perturbation plot, a steep slope or curvature in a decision variable shows that the response is sensitive to that variable. Contrarily, a relatively flat line shows insensitivity. As shown in this figure, because of curvature in lean loading and a steep slope of flue gas inlet temperature into the absorber, these two variables have a significant impact on CO_2 capture cost. This result is consistent with the results of the ANOVA table. According to Table 9, the corresponding F-value of these variables is higher than the others.

As stated before, the CCC is directly proportional with the TAC and inversely with the total mass of captured CO_2. Since in this study, a constant removal rate of 90 % is considered, so the CCC only varies with varying the total annual cost. The TAC itself depends on the TCI and TOC and therefore, lots of variables affect the CCC. Among the various costs affecting the TAC, the energy required for the solvent regeneration, contributes more than 87 % of the TOC and 73 % of the TAC. As a result, it is considered an important and influential factor in the TAC. As seen from Fig. 7, there is an optimal value for α_{lean}, where the CCC becomes minimum. This is mainly related to the regeneration energy, which in a targeted CO_2 removal rate, first decreases and then increases with

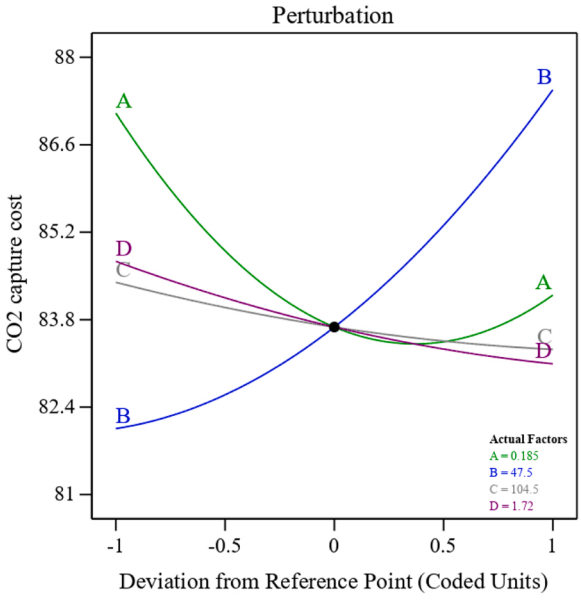

Fig. 7. perturbation plot of all the decision variables.

respect to the lean loading. In the case of flue gas inlet temperature into the absorber, the CCC increases with increasing inlet temperature, while rich amine inlet temperature into the regenerator and regenerator reboiler pressure have a converse effect on the CCC.

4.4. Optimization

In this section, the optimization results of the process operating conditions are discussed. The goal of the optimization in this study is to minimize the CO_2 capture cost. Consequently, the optimum decision variables of the process were carried out by using numerical optimization in the Design Expert v13. To perform optimization, the desired scope for each of the decision variable was chosen "in range", while for the response, it was defined as "minimize". Then the software will search the design space using the created model to find values of variables that meet the defined goal. The optimal operating conditions and the value of the output response are depicted in the ramps graph in Fig. 8. As it can be seen, the optimal variables setting are shown with red points, while the optimal response prediction is displayed in blue. According to the optimization, the minimum value of the CCC equals 80.8727 $\$/t_{CO2}$.

4.5. Energy and economic assesments

Once the optimal working fluid and operating conditions of the whole process are obtained, the economic analysis can be conducted. As stated before, unlike the conventional methods that use DCC, the ORC system was used in this study to reduce the temperature of the flue gas. Hence, it is necessary to make a comparison between these two schemes. It should be noted that the operating conditions of the DCC+CC process are the same as the optimal one for ORC+CC.

The energy performance of the ORC+CC and DCC+CC systems is shown in Table 10. Compared to the optimal ORC+CC system, the equivalent work of the optimal DCC+CC system increases by 28%. The reason is related to the turbine of the ORC that produces power and makes it a reduction in equivalent work of the ORC+CC system.

The global TCI of the optimal process of ORC+CC is estimated at 19.9988 M$, which the TCI related to the ORC system and carbon capture unit and compression is 28.59 % and 71.41 %, respectively. On the other hand, the global TCI for the optimal process of DCC+CC is 15.0844 M$. This difference between these investments is related to the ORC, which is 7.26 times more expensive than the DCC. The contribution of each equipment set to the TCI is shown in Fig. 9(a). As is obvious, the main difference between these two processes is related to the heat exchangers, with 37.44 % of TCI in the ORC+CC belongs to the heat exchangers, while this value reduces to 32.6 % in DCC+CC. This is due to the presence of SHX and condenser in the ORC. In the ORC+CC process, Compressors, columns and turbine are in the subsequent positions of the TCI, respectively. The TCI related to the process vessels, column packings, ORC working fluid, initial MEA solution, and pumps is less than 9 %. In the case of DCC+CC, the compressors set have the highest share of the TCI, followed by heat exchangers and columns. Again, the share of the process vessels, column packings, initial MEA solution, and circulating water and pumps is less than 9 %.

Table 10
energy performance of the optimal ORC+CC and DCC+CC systems.

System	W_{th} (GJ/t_{CO2})	W_c (GJ/t_{CO2})	W_p (GJ/t_{CO2})	$W_{t,ORC}$ (GJ/t_{CO2})	W_{eq} (GJ/t_{CO2})
ORC+CC	0.8282	0.4860	0.02514	0.3309	1.00844
DCC+CC	0.8283	0.4554	0.00709	0	1.29079

The individual contributors to the VOC are depicted in Fig. 9(b). it can be observed that the amine regeneration energy is the main contributor to the VOC, as it accounts for 91.47 % of the ORC+CC system and 86.15 % of the DCC+CC system. This is why, in recent years, many studies have been conducted to reduce amine regeneration energy. The electricity needed to run the rotary equipment contributes 3.71% of the VOC in the ORC+CC, while this value increases to 8.95 % in the DCC+CC. The reason for this huge difference is related to the produced power by the turbine in the ORC+CC process that causes to a reduction of power consumption from the grid.

The most crucial index in assessing the performance of carbon capture units is the CO_2 capture cost. This index can be calculated using Eq. (22). The CCC for the optimal ORC+CC process was evaluated to be

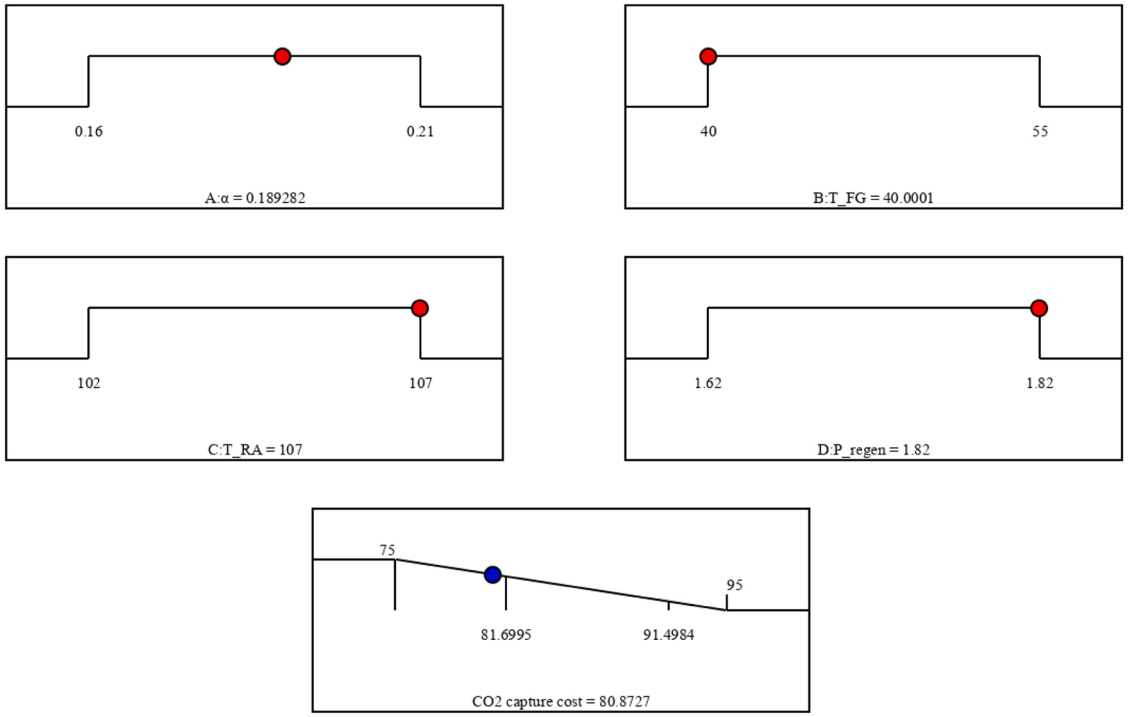

Fig. 8. the optimal operating conditions and corresponding response value of the integrated system.

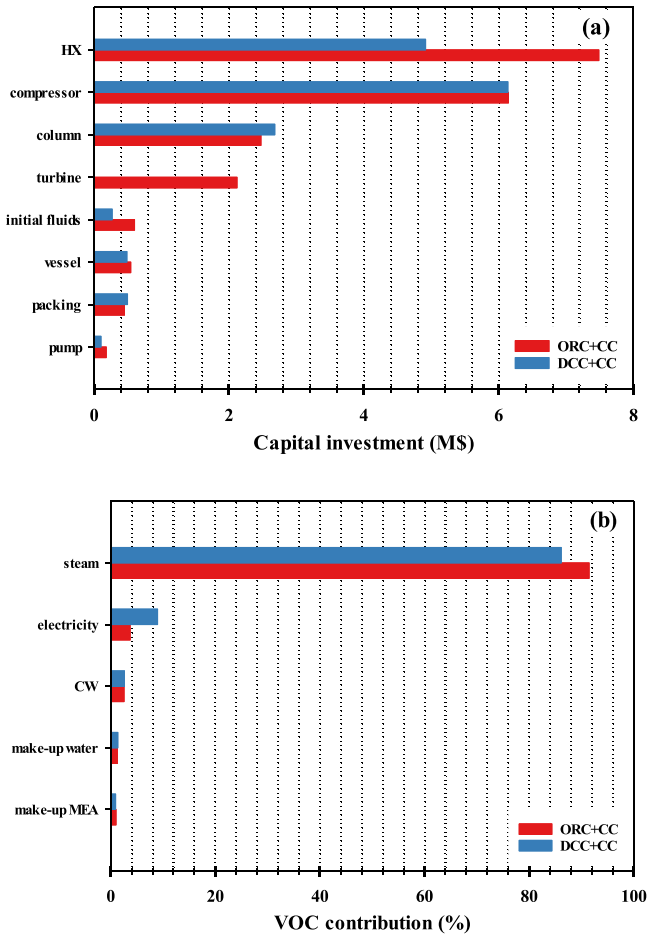

Fig. 9. comparative of ORC+CC and DCC+CC for (a) capital investment, and (b) VOC contribution.

81.60 $/$t_{CO2}$, while for the optimal DCC+CC process, this value is 81.90 $/$t_{CO2}$. These values are higher than the values published in some literature. There are many reasons can explain why the estimated CCC in this study is higher than those reported in some literature. The first reason is related to the size of the system. In the literature, the annual captured CO_2 is relatively higher than in this study (>1,000,000 t_{CO2}/year compared to 153,824 t_{CO2}/year). Based on economics principles, the higher the CO_2 production rate, the lower the CCC. The second reason is the concentration of CO_2 in the flue gas. In the present study, 7.87 mol% of the flue gas is CO_2, which is much lower than that of the literature one (> 18 mol%). The higher the concentration of the CO_2 in the flue gas, the easier capture and the lower the capture cost. Finally, the third reason is attributed to the assumed unit cost of VOCs, especially steam used for MEA regeneration and electricity. Fig. 10 reveals the share of fixed and various variable operating costs together with annualized total capital investment in CCC. As can be seen, the CO_2 capture cost of these two processes is almost equal to each other, as the higher TCI_{annual} and FOC of the ORC+CC process compared to the DCC+CC process is neutralized by the low electricity consumption.

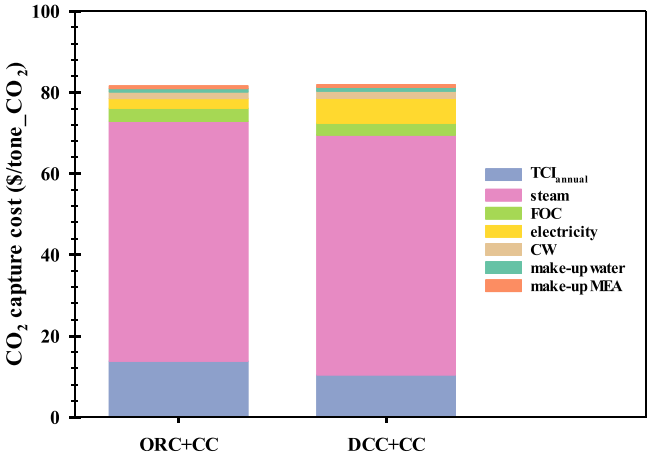

Fig. 10. distributions of CO_2 capture cost.

It was observed that the CO_2 capture cost is almost equal using the ORC+CC or DCC+CC systems. The question that arises here is: what is the benefit and advantage of using the ORC+CC instead of the DCC+CC? to answer this question, two different approaches are presented. The first approach is Saving-to-investment (SIR) indicator. The SIR can be calculated by dividing the savings of TOC during the project lifetime by the changes in the TCI. In other words, the SIR is an indicator between added equipment costs and reduced operating costs. A SIR ratio greater than 1.0 indicates an economically feasible scheme [20]. According to this definition, the value of SIR for the ORC+CC system compared to DCC+CC is equal to 3.353. This high value for the SIR indicates the economic feasibilities of the ORC+CC system.

The second approach is related to fossil fuel consumption and greenhouse gas emissions. The DCC+CC system consumes more electrical power than the ORC+CC system. This electrical power is mainly produced by the combustion of the fossil fuels. So, the ORC+CC system can take the advantage of reducing fossil fuel consumption as well as greenhouse gas emissions. If the ORC plant is used instead of a petroleum-based power plant, the amount of saved petroleum and reduced CO_2 emissions can be estimated by [45]:

$$M_{pe} = hr \times a_{pe} \times W_{net,ORC} \tag{31}$$

$$M_{em} = hr \times a_{em} \times W_{net,ORC} \tag{32}$$

Where hr is the annual operation hour (8160 hr), a_{pe} is the amount of petroleum used to produce 1 kWh of electricity and equals 0.266 (L/kWh). Also, a_{em} is the amount of CO_2 emissions if 1 kWh of electricity is produced by the petroleum-based power plant and equals 0.894 (kg/kWh). In the ORC+CC system, the $W_{net,ORC}$ is equal to 1623.637 kW. Therefore, although the CCC is the same for both ORC+CC and DCC+CC systems, almost 3524.2 m^3/year of petroleum can be saved by using the ORC+CC system. Also, it reduces CO_2 emissions by 11,844.5 t/year.

5. Conclusions

In this paper, a new system that integrates an organic Rankine cycle for waste heat recovery and a post-combustion carbon capture unit for CO_2 emissions reduction with refinery furnaces has been analyzed. The integrated system was simulated in Aspen HYSYS v10 with “Acid Gas - Chemical Solvents” and “Peng-Robinson” fluid packages. Iin the case of ORC, four different working fluid is analyzed to select the suitable one with the optimal condition by using multi-objective optimization. Then, the overall system is optimized by the RSM-BBD method in Design Expert v13 by considering four decision variables. The main results obtained from this study are as follows:

- Among the primary considered working fluids, R-245fa is selected as the suitable one for power generation with a degree of superheating equal to 15.8 °C.
- The results of the ANOVA table imply that the RSM model is significant with a very low probability of error and applicable for optimizing the output response.
- Flue gas inlet temperature into the absorber and lean loading are the most significant terms of the model, respectively.
- The CO_2 capture cost has a direct relationship with the flue gas inlet temperature into the absorber, and an inverse relationship with the

amine inlet temperature into the regenerator and regenerator reboiler pressure. Also, it has a minimum with respect to the lean loading.

- The optimal setting of the decision variables are: $\alpha_{lean} = 0.1893\ mol_{CO2}/mol_{amine}$, $T_{FG} = 40\ ^{\circ}C$, $T_{RA} = 107\ ^{\circ}C$ and $P_{regen} = 1.82$ bar.
- The equivalent work of the optimal ORC+CC system is 21.87 % less than the optimal DCC+CC system.
- In the ORC+CC system, the main contributor of the TCI belongs to the heat exchangers, while for the DCC+CC, it belongs to the compressors.
- The main contributor to the VOC is the steam used for amine regeneration, which equals 91.47 % and 86.15 % for the optimal ORC+CC and optimal DCC+CC, respectively.
- Because of the presence of the turbine in the ORC+CC system, the needed electricity is 58.55 % less than in the DCC+CC system.
- The CCC for the optimal ORC+CC and DCC+CC processes are 81.60 $/t$_{CO2}$ and 81.90 $/t$_{CO2}$, respectively.
- A SIR value of 3.353 for the ORC+CC system compared to the DCC+CC indicates the economic feasibilities of the ORC+CC process.
- By using the ORC+CC system instead of the DCC+CC system, 3524.2 m^3/year of petroleum can be saved and the CO_2 emissions can reduce by 11,844.5 t/year.

CRediT authorship contribution statement

Reza Nazerifard: Investigation, Conceptualization, Writing- Original draft, **Mousa Mohammadpourfard**: Supervision, Verification, Reviewing and Editing, **Saeed Zeinali Heris**: Reviewing and Editing.

Declaration of Competing Interest

The authors declare that they have no known competing financial interests or personal relationships that could have appeared to influence the work reported in this paper.

Data availability

No data was used for the research described in the article.

References

[1] M.F. Hasan, E.L. First, F. Boukouvala, C.A. Floudas, A multi-scale framework for CO_2 capture, utilization, and sequestration: CCUS and CCU, Comput. Chem. Eng. 81 (2015) 2–21.

[2] U.M. Ekanayake, S. Rahmati, R. Zhou, R. Zhou, P.J. Cullen, A.P. O'Mullane, et al., Power-to-decarbonization: mesoporous carbon-MgO nanohybrid derived from plasma-activated seawater salt-loaded biomass for efficient CO_2 capture, J. CO_2 Util. 53 (2021), 101711.

[3] M. Amiri, S. Shahhosseini, A. Ghaemi, Optimization of CO_2 capture process from simulated flue gas by dry regenerable alkali metal carbonate based adsorbent using response surface methodology, Energy Fuels 31 (2017) 5286–5296.

[4] I. Ghiat, T. Al-Ansari, A review of carbon capture and utilisation as a CO_2 abatement opportunity within the EWF nexus, J. CO_2 Util. 45 (2021), 101432.

[5] X.-Q. Wang, X.-P. Li, Y.-R. Li, C.-M. Wu, Payback period estimation and parameter optimization of subcritical organic Rankine cycle system for waste heat recovery, Energy 88 (2015) (734-45).

[6] X. Liang, X. Wang, G. Shu, H. Wei, H. Tian, X. Wang, A review and selection of engine waste heat recovery technologies using analytic hierarchy process and grey relational analysis, Int. J. Energy Res. 39 (2015) (453-71).

[7] Y. Wang, X. Liu, X. Ding, Y. Weng, Experimental investigation on the performance of ORC power system using zeotropic mixture R601a/R600a, Int. J. Energy Res. 41 (2017) (673-88).

[8] M. Leveni, R. Cozzolino, Energy, exergy, and cost comparison of Goswami cycle and cascade organic Rankine cycle/absorption chiller system for geothermal application, Energy Convers. Manag. 227 (2021), 113598.

[9] S. Wang, C. Liu, S. Zhang, Q. Li, E. Huo, Multi-objective optimization and fluid selection of organic Rankine cycle (ORC) system based on economic-environmental-sustainable analysis, Energy Convers. Manag. 254 (2022), 115238.

[10] A. Behzadi, E. Gholamian, E. Houshfar, A. Habibollahzade, Multi-objective optimization and exergoeconomic analysis of waste heat recovery from Tehran's waste-to-energy plant integrated with an ORC unit, Energy 160 (2018), 1055-68.

[11] Y. Jin, N. Gao, T. Zhu, Techno-economic analysis on a new conceptual design of waste heat recovery for boiler exhaust flue gas of coal-fired power plants, Energy Convers. Manag. 200 (2019), 112097.

[12] S.M. Safdarnejad, J.D. Hedengren, L.L. Baxter, Plant-level dynamic optimization of cryogenic carbon capture with conventional and renewable power sources, Appl. Energy 149 (2015) (354-66).

[13] C. Ji, S. Yuan, M. Huffman, M.M. El-Halwagi, Q. Wang, Post-combustion carbon capture for tank to propeller via process modeling and simulation, J. CO_2 Util. 51 (2021), 101655.

[14] P. Talebizadehsardari, M. Ehyaei, A. Ahmadi, D. Jamali, R. Shirmohammadi, A. Eyvazian, et al., Energy, exergy, economic, exergoeconomic, and exergoenvironmental (5E) analyses of a triple cycle with carbon capture, J. CO_2 Util. 41 (2020), 101258.

[15] A. Sharif, A. Jahangiri, M. Ameri, CO_2 capturing from flue gases injected into the NDDCT: feasibility study, exergy and economic investigation of simultaneously MEA-solvent chemical absorption and flue gas injection, Sustain. Energy Technol. Assess. 45 (2021), 101102.

[16] S.M. Hosseini-Ardali, M. Hazrati-Kalbibaki, M. Fattahi, F. Lezsovits, Multi-objective optimization of post combustion CO_2 capture using methyldiethanolamine (MDEA) and piperazine (PZ) bi-solvent, Energy 211 (2020), 119035.

[17] S. Seo, B. Lages, M. Kim, Catalytic CO_2 absorption in an amine solvent using nickel nanoparticles for post-combustion carbon capture, J. CO_2 Util. 36 (2020) (244-52).

[18] J. Bravo, D. Drapanauskaite, N. Sarunac, C. Romero, T. Jesikiewicz, J. Baltrusaitis, Optimization of energy requirements for CO_2 post-combustion capture process through advanced thermal integration, Fuel 283 (2021), 118940.

[19] O. Otitoju, E. Oko, M. Wang, Technical and economic performance assessment of post-combustion carbon capture using piperazine for large scale natural gas combined cycle power plants through process simulation, Appl. Energy 292 (2021), 116893.

[20] H.-T. Oh, Y. Ju, K. Chung, C.-H. Lee, Techno-economic analysis of advanced stripper configurations for post-combustion CO_2 capture amine processes, Energy 206 (2020), 118164.

[21] L. Dubois, D. Thomas, Comparison of various configurations of the absorption-regeneration process using different solvents for the post-combustion CO_2 capture applied to cement plant flue gases, Int. J. Greenh. Gas. Control 69 (2018) 20–35.

[22] M. Sharma, F. Parvareh, A. Abbas, Highly integrated post-combustion carbon capture process in a coal-fired power plant with solar repowering, Int. J. Energy Res. 39 (2015) 1623–1635.

[23] C. Nwaoha, M. Beaulieu, P. Tontiwachwuthikul, M.D. Gibson, Techno-economic analysis of CO_2 capture from a 1.2 million MTPA cement plant using AMP-PZ-MEA blend, Int. J. Greenh. Gas. Control 78 (2018) (400-12).

[24] S.K. Dash, A.N. Samanta, S.S. Bandyopadhyay, Simulation and parametric study of post combustion CO_2 capture process using (AMP+ PZ) blended solvent, Int. J. Greenh. Gas. Control 21 (2014) 130–139.

[25] R. Zhang, X. Zhang, Q. Yang, H. Yu, Z. Liang, X. Luo, Analysis of the reduction of energy cost by using MEA-MDEA-PZ solvent for post-combustion carbon dioxide capture (PCC), Appl. Energy 205 (2017) (1002-11).

[26] J. Jung, Y.S. Jeong, U. Lee, Y. Lim, C. Han, New configuration of the CO_2 capture process using aqueous monoethanolamine for coal-fired power plants, Ind. Eng. Chem. Res. 54 (2015) 3865–3878.

[27] B. Zhao, F. Liu, Z. Cui, C. Liu, H. Yue, S. Tang, et al., Enhancing the energetic efficiency of MDEA/PZ-based CO_2 capture technology for a 650 MW power plant: process improvement, Appl. Energy 185 (2017), 362-75.

[28] C. Nwaoha, D.W. Smith, R. Idem, P. Tontiwachwuthikul, Process simulation and parametric sensitivity study of CO_2 capture from 115 MW coal–fired power plant using MEA–DEA blend, Int. J. Greenh. Gas. Control 76 (2018) 1–11.

[29] M.R. Abu-Zahra, L.H. Schneiders, J.P. Niederer, P.H. Feron, G.F. Versteeg, CO_2 capture from power plants: Part I. A parametric study of the technical performance based on monoethanolamine, Int. J. Greenh. Gas. Control 1 (2007) 37–46.

[30] S. Wang, C. Liu, Q. Li, L. Liu, E. Huo, C. Zhang, Selection principle of working fluid for organic Rankine cycle based on environmental benefits and economic performance, Appl. Therm. Eng. 178 (2020), 115598.

[31] B.F. Tchanche, G. Lambrinos, A. Frangoudakis, G. Papadakis, Low-grade heat conversion into power using organic Rankine cycles – a review of various applications, Renew. Sustain. Energy Rev. 15 (2011), 3963-79.

[32] R. Nazerifard, L. Khani, M. Mohammadpourfard, B. Mohammadi-Ivatloo, G. G. Akkurt, Design and thermodynamic analysis of a novel methanol, hydrogen, and power trigeneration system based on renewable energy and flue gas carbon dioxide, Energy Convers. Manag. 233 (2021), 113922.

[33] M. Naveiro, M.R. Gómez, I. Arias-Fernández, Á.B. Insua, Thermodynamic and environmental analyses of a novel closed loop regasification system integrating ORC and CO_2 capture in floating storage regasification units, Energy Convers. Manag. 257 (2022), 115410.

[34] M. Karimi, M. Hillestad, H.F. Svendsen, Capital costs and energy considerations of different alternative stripper configurations for post combustion CO_2 capture, Chem. Eng. Res. Des. 89 (2011), 1229-36.

[35] R. Turton, R.C. Bailie, W.B. Whiting, J.A. Shaeiwitz, Analysis synthesis and design of chemical processes, Pearson Educ. (2008).

[36] M. Astolfi, M.C. Romano, P. Bombarda, E. Macchi, Binary ORC (Organic Rankine Cycles) power plants for the exploitation of medium–low temperature geothermal sources–Part B: techno-economic optimization, Energy 66 (2014), 435-46.

[37] A.K. Coker, Ludwig's Applied Process Design for Chemical and Petrochemical Plants, fourth ed., Gulf Professional Publishing, 2015.

[38] H. Jilvero, A. Mathisen, N.-H. Eldrup, F. Normann, F. Johnsson, G.I. Müller, et al., Techno-economic analysis of carbon capture at an aluminum production

plant–comparison of post-combustion capture using MEA and ammonia, Energy Procedia 63 (2014) (6590-601).
[39] S. Georgousopoulos, K. Braimakis, D. Grimekis, S. Karellas, Thermodynamic and techno-economic assessment of pure and zeotropic fluid ORCs for waste heat recovery in a biomass IGCC plant, Appl. Therm. Eng. 183 (2021), 116202.
[40] F. Yang, H. Cho, H. Zhang, J. Zhang, Thermoeconomic multi-objective optimization of a dual loop organic Rankine cycle (ORC) for CNG engine waste heat recovery, Appl. Energy 205 (2017) (1100-18).
[41] C. Nwaoha, P. Tontiwachwuthikul, Carbon dioxide capture from pulp mill using 2-amino-2-methyl-1-propanol and monoethanolamine blend: Techno-economic assessment of advanced process configuration, Appl. Energy 250 (2019), 1202-16.
[42] N. Kazemi, F. Samadi, Thermodynamic, economic and thermo-economic optimization of a new proposed organic Rankine cycle for energy production from geothermal resources, Energy Convers. Manag. 121 (2016) 391–401.
[43] S. Safarian, F. Aramoun, Energy and exergy assessments of modified organic rankine cycles (ORCs), Energy Rep. 1 (2015) 1–7.
[44] R. Notz, H.P. Mangalapally, H. Hasse, Post combustion CO_2 capture by reactive absorption: pilot plant description and results of systematic studies with MEA, Int. J. Greenh. Gas. Control 6 (2012) 84–112.
[45] Z. Shengjun, W. Huaixin, G. Tao, Performance comparison and parametric optimization of subcritical organic rankine cycle (ORC) and transcritical power cycle system for low-temperature geothermal power generation, Appl. Energy 88 (2011) (2740-54).